Colloids and Surfaces A: Physicochem. Eng. Aspects 460 (2014) 386–390

Contents lists available at ScienceDirect

Colloids and Surfaces A: Physicochemical and Engineering Aspects

journal homepage: www.elsevier.com/locate/colsurfa

Analysis of bubble-in-liquid bridge configuration as prototype for studying foam dynamics. Zero Bond number case

M. Kostoglou*, T.D. Karapantsios

Department of Chemical Technology, School of Chemistry, Aristotle University, Univ. Box 116, 541 24 Thessaloniki, Greece

HIGHLIGHTS

- Theoretical study of bubble in liquid bridge problem for zero Bond number.
- Existence of two bridge rupture mode: neck rupture and film rupture.
- Existence of an optimum bubble size for maximizing bridge stability.

GRAPHICAL ABSTRACT

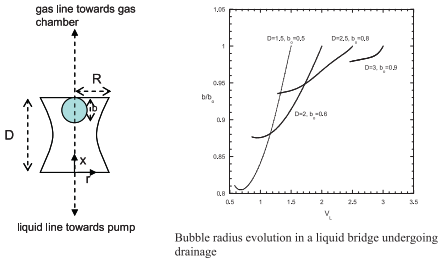

Bubble radius evolution in a liquid bridge undergoing drainage

ARTICLE INFO

Article history:
Received 29 October 2013
Received in revised form
20 December 2013
Accepted 23 December 2013
Available online 1 January 2014

Keywords:
Bubble in liquid bridge
Theoretical analysis
Zero Bond number
Bridge rupture film rupture
Neck rupture

ABSTRACT

A bubble-in-liquid bridge is a unique configuration that resembles the case of two neighboring bubbles in a foam separated by a liquid layer. It calls for a small bubble inside a liquid bridge with the curved free surface of the liquid bridge acting as part of a larger external bubble. This configuration can serve as a prototype to study foam dynamics. A devise exploring this concept has been presented in a previous work (Kostoglou et al., 2011). The present work adds to the theoretical background of the proposed devise. The particular case of zero Bond number is studied theoretically here. Even in its simplest form the particular system exhibits an interesting behavior. It is shown that there are two rupture modes of the liquid bridge as the liquid volume decreases i.e. neck rupture and film rupture. The prevailing one depends on system parameters. The evolution of the bubble size as the liquid volume decreases up to rupture, is extensively studied.

1. Introduction

Liquid bridges formed between solid surfaces have been the study of extensive research through the last 100 years. The main reason is that apart of the fundamental importance of the subject, there are a variety of applications involving liquid bridges. For example, liquid bridges between particles are important in particulate processes such as granulation, flotation, coating [1,2]. They are also important for moist soil properties [3]. Another family of applications regards the production of high quality crystals [4], alignment of components using optoelectronics assemblies, and the control of forces in microgripping processes [5]. Study of the above processes requires the knowledge of the bridge shape which is dictated by the well-known Young–Laplace equation. In general, this equation does not have analytical solution so a large amount of literature is devoted to derivation of approximate solutions of this equation that offer physical insight and facilitate interpretation of experimental data [6–11].

Several designs based on quasi-static or dynamic liquid bridges have been proposed as tools for studying static or dynamic surface properties [12,13]. Traditionally, liquid bridges have been studied either by measuring the force exerted by the liquid bridge to its supporting boundaries or using image processing techniques to

* Corresponding author. Tel.: +30 2310997767; fax: +30 2310997759.
E-mail address: kostoglu@chem.auth.gr (M. Kostoglou).

0927-7757/$ – see front matter © 2014 Elsevier B.V. All rights reserved.
http://dx.doi.org/10.1016/j.colsurfa.2013.12.045

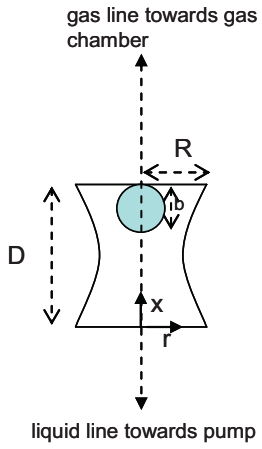

Fig. 1. Schematic of the liquid bridge-bubble system.

identify the liquid bridge profile. In both cases, a usual goal was to estimate surface tension or contact angle from liquid bridge characteristics. However, both techniques require excessive skill and are cumbersome. The apparent electrical conductance of conducting liquid bridges has been suggested as an alternative characteristic parameter from which liquid bridge features can be directly deduced [12,14]. Recently, a configuration consisting of a bubble-in-liquid bridge has been proposed to examine the surfactant induced stabilization of the liquid layer between the internal bubble and the external free surface of the bridge as the liquid was draining out of the bridge [14]. An advantage of this configuration is that the stability of the liquid layer can be followed continuously starting from an appreciable thickness of the layer down to a very thin film up to the rupture point. Ultra-sensitive electrical conductance measurements were employed to follow the drainage of a liquid bridge pinned at the rims of flat rod electrodes. Electrical signals can easily sense liquid films of the order of microns or less without the complications of optical distortion and focusing of traditional imaging techniques. The analysis performed in [14] was based on the assumption of a constant bubble size during liquid drainage. This assumption is relaxed in the present work by considering an evolving bubble size during drainage.

The scope of the present study is the fundamental analysis of the configurations of the bubble-in-liquid bridge system during liquid volume reduction (drainage of the bridge) in the absence of surfactant and for zero Bond number. In the next section the mathematical problem is formulated and the behavior of its solution with emphasis to the evolution of the bubble size is discussed in the results section.

2. Problem formulation

The geometry of the problem is shown in Fig. 1. A liquid bridge is edge-pinned between the tips of two equal diameter solid rods which are aligned vertically. Both rods have tiny holes at their center. These holes have diameters an order of magnitude smaller than the diameter of the rods. The hole at the top rod is meant to create an internal bubble to the bridge by blowing air through it whereas the hole at the bottom rod is meant for draining the bridge liquid. The internal bubble is connected to an air chamber. From the practical point of view the air chamber is necessary for creating the bubble and measuring is internal pressure. The pressure and volume in the chamber is adjusted to achieve a bubble of the desired size. The issue of interest here is to study the evolution of the liquid bridge shape, the bubble size and the pressure in the liquid during liquid withdrawal. The study will be performed for conditions that correspond to the following assumptions.

(i) The liquid is a pure liquid with surface tension γ. There are no surfactants in the system for surface tension manipulation. Surfactant through their adsorption/desorption on interfaces and diffusion adds significant complexity to the problem and cannot be taken into account by simply altering the equilibrium surface tension [15].
(ii) The whole process occurs under constant temperature conditions and 100% relative humidity to prevent evaporation.
(iii) The effect of gravity can be ignored (negligibly small value of the Bond number). This condition is met in three situations (based on different ways to decrease Bo): microgravity environment, small dimensions of the liquid bridge, replacing the external air by another immiscible liquid whose density matches the density of the bridge liquid.
(iv) Rod material fully wetted by the bridge liquid. This assumption combined with (i) and (iii) ensures that the shape of the internal bubble is always spherical.
(v) The gas is insoluble in the liquid. This assumption is needed to exclude the Ostwald ripening phenomenon i.e. the bubble dissolution due to its higher pressure than the environment pressure.
(vi) The liquid withdrawal flowrate is relatively small to ensure that the viscous stresses are negligibly small compared to the surface tension forces and the bridge shape can be determined by pseudo-steady energy balance (i.e. Young–Laplace equation). This assumption implies that the liquid flow rate does not alter the evolution path of the system but simply influences the time variable. The state of the system is fully determined by its liquid content which can be used as the time-like evolution variable.

Considering a cylindrical coordinate system x, r with its center at the center of the bottom rod and denoting as R the rod radius, D the liquid bridge length (height), V_{Lo} the initial liquid volume, V_L the instantaneous liquid volume, b_o the initial internal bubble radius, b the instantaneous internal bubble radius, V_c the volume of the air chamber connected with the bubble, P_o the environmental pressure and $r = Y(x)$ the shape of the liquid bridge, the problem is described from the following set of equations:

Young–Laplace equation for the liquid bridge shape

$$\left(1+\left(\frac{dY}{dx}\right)^2\right)^{-3/2}\left[-\frac{d^2Y}{dx^2}+\frac{1}{Y}\left(1+\left(\frac{dY}{dx}\right)^2\right)\right]=\frac{\Delta P}{\gamma} \tag{1}$$

where $\Delta P = P_L - P_o$ is the pressure difference between the liquid bridge and the environment due to the curvature of the liquid bridge. The boundary conditions for the above second order boundary value problem are

$$Y(0) = R, \tag{2a}$$

$$Y(D) = R \tag{2b}$$

The additional unknown parameter ΔP is found from the requirement of liquid volume conservation:

$$V_L = \pi \int_0^D [Y^2(x) - U(b^2 - (x - D + b)^2)]\, dx \tag{3}$$

where the function U is defined as $U(x) = 0$ for $x < 0$ and $U(x) = x$ for $x \geq 0$.

The above mathematical problem can be solved for the instantaneous liquid bridge shape for a given bubble diameter b. An evolution equation for the bubble radius is needed and it is based on the requirement that the mass of gas in the domain defined by the

gas chamber and the bubble remains constant during the shrinkage of the liquid bridge (based on assumption (ν) regarding gas solubility). Taking into account that the pressure in the spherical bubble is $P_b = P_L + 2\gamma/b$ the above condition can be written as:

$$P_b(V_c + V_b) = \left(P_o + \Delta P + \frac{2\gamma}{b}\right)(V_c + V_b) = \text{constant} \tag{4}$$

where V_b is the instantaneous bubble volume. The constant can be determined from the initial state of the system so the evolution equation takes the form

$$\left(\left(P_o + \Delta P + \frac{2\gamma}{b}\right)\left(V_c + \frac{4}{3}\pi b^3\right)\right) = \left(P_o + \Delta P_o + \frac{2\gamma}{b_o}\right)\left(V_c + \frac{4}{3}\pi {b_o}^3\right) \tag{5}$$

where ΔP_o is the initial value of ΔP. The problem contains several physical parameters and it is important to gather them in dimensionless groups through a proper non-dimensionalization. The same symbols will be retained for the dimensionless variables for clarity of presentation. This will be not confusing since in the following only dimensionless variables appear. The length variables D, b, b_o are normalized by the rod radius R. The volume variables V_L, V_b, V_{bo} are normalized with respect to πR^3. The overpessure ΔP in the bridge is nondimensionalized introducing the new variable $H = R\Delta P/\gamma$. The second order Eq. (1) is transformed to a system of two first order equations which greatly facilitates the numerical treatment of the problem [16]. A new independent variable, Φ, appears representing the external angle between the bridge shape and the horizontal level. The dimensionless problem takes the form:

$$\frac{d\Phi}{dx} = \frac{H}{\sin(\Phi)} - \frac{1}{Y} \tag{6}$$

$$\frac{dY}{dx} = \frac{1}{\tan(\Phi)} \tag{7}$$

$$Y(0) = 1 \tag{8a}$$

$$Y(D) = 1 \tag{8b}$$

$$V_L = \int_0^D [Y^2(x) - U(b^2 - (x - D + b)^2)]dx \tag{9}$$

$$\left(A + H + \frac{2}{b}\right)(1 + Bb^3) = \left(A + H_o + \frac{2}{b_o}\right)(1 + Bb_o^3) \tag{10}$$

The dimensionless parameters A, B are defined as:

$$A = \frac{P_o R}{\gamma} \tag{11}$$

$$B = \frac{4\pi R^3}{V_c} \tag{12}$$

where A denotes the ratio of the environment pressure to the curvature induced pressure and B is a normalized inverse gas chamber volume.

The above is clearly an evolution problem with V_L being the evolution time-like variable. Starting with initial condition $b = b_o$ at $V_L = V_{Lo}$ the problem must be solved for the evolution of $Y(x)$, H and b as V_L decreases up to the bridge rupture volume V_{Lr}. The problem parameters apart of the initial conditions are D, A and B. The numerical solution algorithm is based on (i) transformation of (9) to an ordinary differential equation, (ii) numerical integration of (6), (7) and (9) as initial value problem and (iii) perform shooting method using the Newton–Raphson method to find $\Phi(0)$ and H that fulfils the volume constraint and $Y(D) = 1$. The value of V_L is reduced by very small steps and the above procedure is repeated at any value of V_L using as initial guesses for the Newton–Raphson iterations the converged values at the previous V_L value in order to ensure convergence. The algorithm failure to converge is an indication that V_{Lr} has been reached. The total bridge volume (liquid + bubble) at the moment of rupture is denoted as V_r ($=V_{Lr} + V_b$).

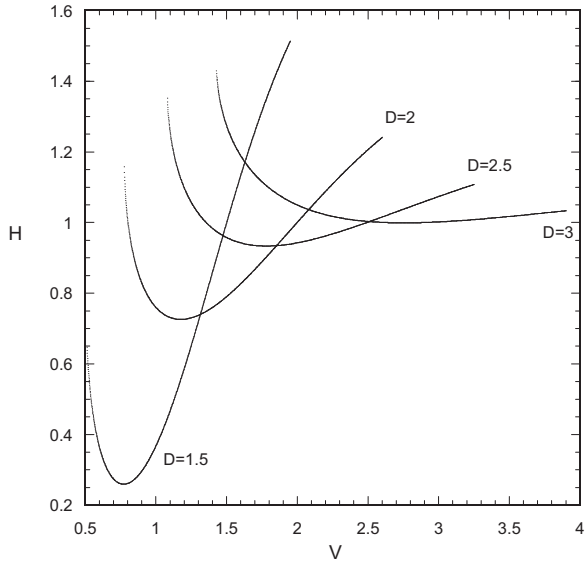

Fig. 2. Dependence of liquid bridge pressure H on total bridge volume V for several values of length D.

3. Results

3.1. Fixed bubble size

The simplest case is to assume a bubble of fixed size during the bridge drainage and shrinkage (i.e. corresponding to $A \gg 1$). The numerical results showed (against the physical intuition) that the liquid bridge shape is always symmetric and there is no longitudinal distortion of the bridge shape associated with the bubble presence. This implies that the liquid bridge shape does not depend on the liquid volume and the bubble size/position independently but only through the total effective bridge volume $V = V_L + V_b$. A confirmation can be made by a careful examination of the governing equations.

From the mathematical point of view the volume conservation condition can be replaced by

$$V = \int_0^D Y^2(x)dx \tag{13}$$

and the system of Eqs. (6), (7) and (13) can produce all the possible liquid bridge shapes as V decreases. It is noted that both Eqs. (9) and (13) are of general validity (the first refer to the bridge liquid volume and the second to the total bridge volume including liquid and a bubble). The only parameter of this problem is the bridge length D. The evolution of the dimensionless bridge overpressure H with respect to the total bridge volume for several values of D (for which stable bridges exist) is shown in Fig. 2. It is interesting how decisive is the bridge length to the pressure evolution as the total volume decreases.

It is chosen for the curves in Fig. 2 to start from a total volume 30% larger than the one corresponding to a cylindrical shape. The initial overpressure is exclusively due to the transverse curvature component. One can easily confirm that the value $H = 1$ that corresponds to the cylindrical shape intersects each curve of Fig. 2 at $V = D$. As the total volume of the bridge decreases further from the

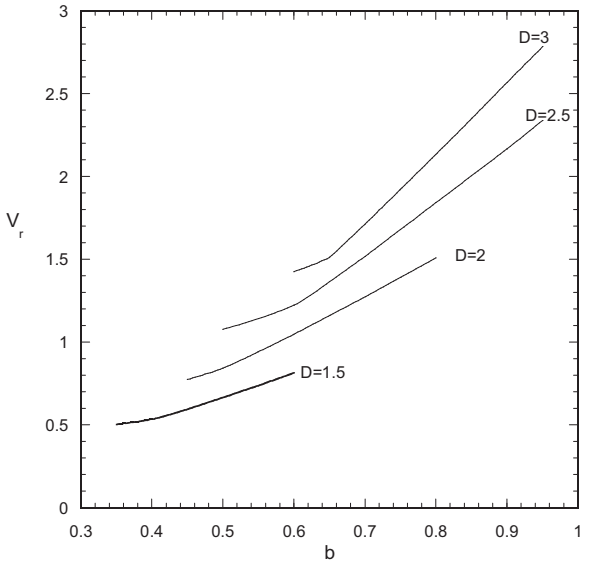

Fig. 3. Total bridge volume V_r at the rupture point vs bubble radius b for several values of length D.

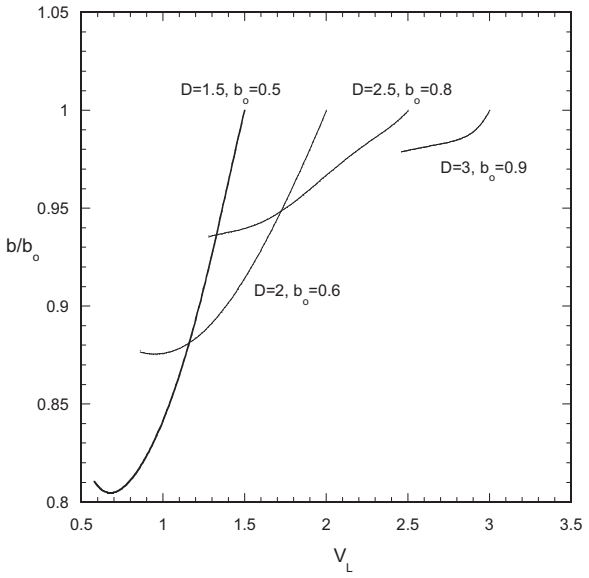

Fig. 4. Evolution of the bubble radius b vs liquid volume V_L for several pairs of length D and initial bubble radius b_o in the limit $B \gg 1$.

cylindrical shape the transverse curvature increases but a longitudinal curvature appears with opposite sign (the liquid is at the concave side). This results to a reduction of the overpressure until V approaches V_r where an abrupt increase of H occurs due to the further increase of the transverse curvature. The above two regions contribute at a different degree to the overall overpressure curve depending on the value of D. For example, the shortest bridge allows the development of large longitudinal curvature leading to almost monotonic H reduction with V reduction. On the other hand, the large length of the bridge for $D = 3$ does not allow development of a significant longitudinal curvature and the part of the curve in which H decreases as V_L decreases almost vanishes.

Each H value along the curves in Fig. 2 corresponds to a particular liquid bridge profile. These curves are taken at the absence of bubble but they still hold (together with the corresponding bridge shapes) at the presence of bubble by simply replacing V by $V_L + V_b$. This similarity does not hold, though, for the V_r values shown in the figure. At each V value and for a specific bubble size b, checking for intersection between the bubble and the bridge surface is needed. The volume at which the bridge free surface tangents the bubble is the real rupture volume V_r which is function of bubble radius b.

So far it is shown that for a particular D value, H and $Y(x)$ depend only on the total volume V but the rupture volume V_r depends explicitly on bubble radius. The dependence of V_r on bubble radius, b, for the four values of D under consideration is shown in Fig. 3. The curves start at a critical bubble radius b_m. For values of $b < b_m$ the bubble never intersects with the bridge free surface and V_r does not depend on bubble size. For bubble radius $b > b_m$ a transition occurs and V_r starts increasing with bubble size. From the physical point of view, for $b < b_m$ the rupture of the bridge occurs with the same mechanism as in the absence of bubble (i.e. absence of solution of the Young–Laplace equation, henceforth referred to as neck rupture) but for $b > b_m$ the rupture occurs due to the thinning of the liquid film created between the bubble and the bridge free surface (henceforth referred to as film rupture). For $b < b_m$ it is $V_r = V_r(D)$ so $V_{Lr} = V_r(D) - V_b$ and it is clear that the existence of a bubble stabilizes the bridge (as b increases neck rupture occurs at smaller liquid volume). For $b > b_m$ $V_r = V_r(D,b)$ and the dependence is such that the liquid rupture volume increases as b increases. So, for bubble size $b = b_m$ the liquid rupture volume reaches its minimum value V_{Lrm}.

3.2. Evolving bubble size

The system bubble-in-bridge for a fixed bubble size and for specified D is completely described by the functions $H(V)$ and $V_r(b)$. In the general case, however, the pressure variation H in the bridge leads to a variation of the bubble size. The behavior of the system during liquid withdrawal is still described by $H(V)$ and $V_r(b)$ but an additional relation between b and V_L exists (Eq. (10)) which determines the evolution of b. The evolution of b depends on the parameters A and B that appear in Eq. (10). Substitution of $H(V)$ in (10) leads to an algebraic equation relating V_L and b that must be solved for the construction of the $b(V_L)$. The point of rupture will not arise from the solution of this equation which continues even after the rupture point but it must be determined by the independent condition $V = V_r(b)$.

Two limiting cases of the Eq. (10) will be examined: In the first case, the bubble volume is negligible compared to the gas chamber volume and the bubble size variation is determined from the requirement for a constant internal bubble pressure. Then Eq. (10) is transformed to

$$H\left(V_L + \frac{4}{3}b^3\right) + \frac{2}{b} = H\left(V_{Lo} + \frac{4}{3}b_o^3\right) + \frac{2}{b_o} \quad (14)$$

i.e. the evolution of the bubble size does not depend on the parameters A, B. This particular case sets up the upper limit in bubble size variation during liquid withdrawal. The evolution of the normalized bubble size for four values of D starting from relatively large bubble size b_o and with an initial liquid quantity corresponding to a cylindrical bridge ($V_L = D$) is shown in Fig. 4. The bubble size variation is larger for smaller values of D. Small bubbles are slightly sensitive to liquid pressure variation. On the other hand, larger bubbles are more sensitive but they accelerate the rupture of the bridge reducing the overall variation in bubble size during liquid withdrawal. The branch of increasing H prior to rupture appearing in Fig. 2 does not appear in bubble size variation in Fig. 4 due to the acceleration of rupture induced by the large bubbles considered.

In order to understand better the influence of the initial bubble size b_o on the evolution of bubble radius for $D = 2$ and several values of b_o are shown in Fig. 5. The curves correspond to the solutions of Eq. (14) which does not take into account the rupture of the bridge. The liquid rupture volume V_{Lr} is represented by the crosses. The crosses correspond to the curve with $D = 2$ in Fig. 3 versus V_{Lr}

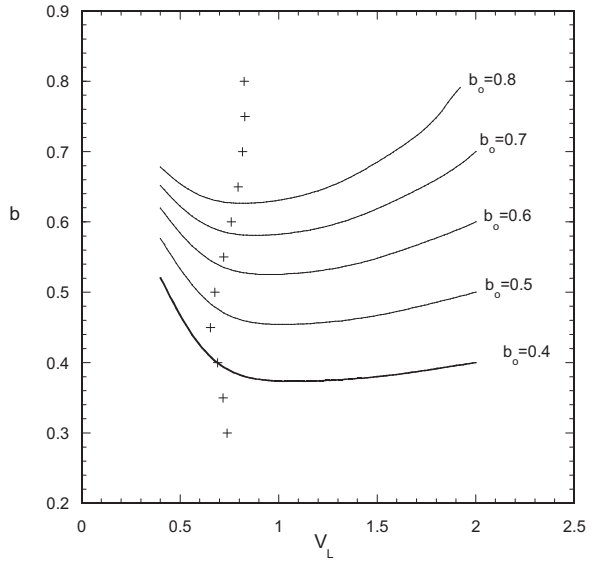

Fig. 5. Evolution of the bubble radius b vs liquid volume V_L for $D = 2$ and several values of initial bubble radius b_o in the limit $B \gg 1$. The crosses designated the rupture location.

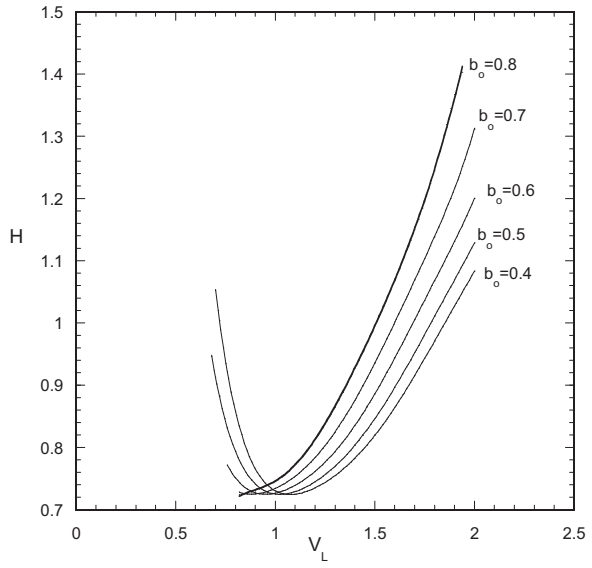

Fig. 6. Evolution of pressure H in the bridge vs liquid volume V_L for $D = 2$ and several values of initial bubble radius b_o in the limit $B \gg 1$.

instead of V_r. The existence of a bubble size with the minimum V_{Lr} is evident. In addition, the increased sensitivity of the bubble with respect to V_L due to liquid pressure, as b_o increases is clearly shown. It is noticed that the increase of bubble radius leads to an increase of V_{Lr} for $b_o > 0.5$.

Fig. 6 displays the evolution of the pressure H for the same cases shown in Fig. 5 to show the effect of the bubble on the liquid bridge pressure. The curves resulted by transformation of the horizontal axis of the curve $D = 2$ in Fig. 2. As b_o increases the difference in shape with respect to the basic curve in Fig. 2 increases. A large bubble prevents the pressure increase prior to rupture.

In the limit $B \gg 1$ (absence of gas chamber) Eq. (10) takes the form

$$\left(A + H + \frac{2}{b}\right) b^3 = \left(A + H_o + \frac{2}{b_o}\right) b_o^3 \qquad (15)$$

The bubble size evolution in this case depends on the parameter A and it is dominated by the bubble compression/expansion process. For rods radius of practical value (i.e. larger than 100 μm) A is of the order of 100 and the variation in b resulting from Eq. (15) is less than 1/100.

In general for any values of A and B the variation of b is smaller than the limiting case $B = 0$ analyzed in detail in the present work. The findings of the present work will allow the assessment of the error in assuming constant bubble size during liquid drainage [14] and the relaxation of this assumption in future studies of employing bubble in liquid bridge device to estimate surface properties.

4. Conclusions

The evolution of a bubble-in-liquid bridge configuration during bridge drainage/shrinkage in the limit of zero Bond number is considered here. It is shown that the complete mathematical problem can be decomposed into simpler subproblems that share the problem parameters. In this way the solution can be presented in a hierarchical way. The liquid bridge shape does not depend on the presence of the internal bubble but only on the sum of liquid and bubble volume. The bubble explicitly affects the liquid volume at the rupture moment. Small bubbles stabilize (neck rupture) and large bubbles destabilize (film rupture) the bridge leading to a specific bubble size at which transition from neck rupture to film rupture mode occurs and which gives the maximum stability to the bridge (minimum liquid volume for a given bridge length). The bubble size evolution can be described by a single algebraic equation. Depending on the system parameters bubble size can be considerably reduced during bridge drainage/shrinkage. The effect of bubble size reduction on the bridge stability depends on the initial bubble size.

Acknowledgment

This work was performed under the umbrella of COST-Action MP-1106 “Smart and Green Interfaces”.

References

[1] S.J.R. Simons, J.P.K. Sevile, M.J. Adams, Chemical Engineering Science 49 (1994) 2331–2339.
[2] P.R. Mort, Powder Technology 150 (2005) 86–103.
[3] F. Molencamp, A.H. Nazemi, Geotechnique 53 (2003) 255–265.
[4] H.C. Kuhlmann, Thermocapillary Convection in Models of Crystal Growth, Springer Verlang, Berlin, 1999.
[5] S. Chadra, C. Batur, Engineering Applications of Computational Mechanics 4 (2010) 181–195.
[6] P.A. Kralchevsky, I.B. Ivanov, A.D. Nikolov, Journal of Colloid and Interface Science 112 (1986) 108–121.
[7] P.A. Kralchevsky, A.S. Dimitrov, K. Nagayama, Journal of Colloid and Interface Science 160 (1993) 236–242.
[8] S. Evgenidis, M. Kostoglou, D. Karapantsios, Journal of Colloid and Interface Science 302 (2006) 597–604.
[9] D. Megias-Alguacil, L. Gauckler, Powder Technology 198 (2010) 211–218.
[10] D. Megias-Alguacil, L. Gauckler, AIChE Journal 55 (2009) 1103–1109.
[11] H. Chen, A. Amirfazli, T. Tang, Langmuir (2013), http://dx.doi.org/10.1021/la304870h (in press).
[12] M. Kostoglou, T.D. Karapantsios, Journal of Colloid and Interface Science 227 (2000) 282–290.
[13] V. Luengo, J. Meseguer, I.E. Parra, Experiments in Fluids 34 (2003) 412–417.
[14] M. Kostoglou, E. Georgiou, T.D. Karapantsios, A. Colloids Surfaces, Colloids and Surfaces A: Physicochemical and Engineering Aspects 382 (2011) 64–73.
[15] V.B. Fainerman, E.V. Aksenenko, J.T. Petkov, R. Miller, Colloids and Surfaces A: Physicochemical and Engineering Aspects 385 (2011) 139–143.
[16] C. Pozrikidis, Fluid dynamics: Theory, Computation and Numerical Simulation, Kluwer, Boston, 2001.